

Supplementary Information

Mononuclear Co(II) polypyridyl complexes: synthesis, molecular structure, DNA binding/cleavage, radical scavenging, docking studies and anticancer activities

Kalai Selvan Karumban^{a†}, Arabinda Muley^{a†}, Rajnikant Raut^b, Parth Gupta^b, Bishnubasu Giri^a,
Sadananda Kumbhakar^a, Ashish Misra^{b*} and Somnath Maji^{a*}

*^aDepartment of Chemistry, Indian Institute of Technology, Hyderabad, Kandi, Sangareddy
502284*

Telangana, India

E-mail: smaji@chy.iith.ac.in

*^bDepartment of Biotechnology, Indian Institute of Technology, Hyderabad, Kandi,
Sangareddy 502284*

Telangana, India

E-mail: ashishmisra@bt.iith.ac.in

† These authors contributed equally to this work.

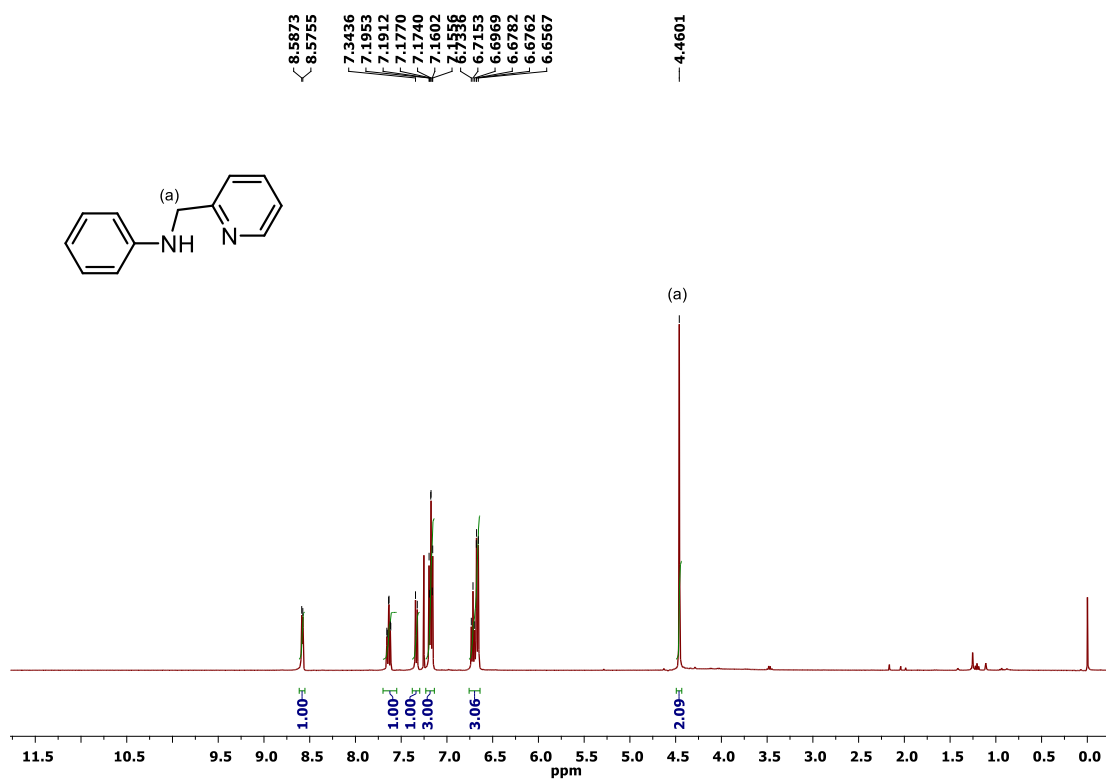


Fig. S1. ¹H NMR of N-(pyridin-2-ylmethyl)aniline in CDCl₃ at room temperature.

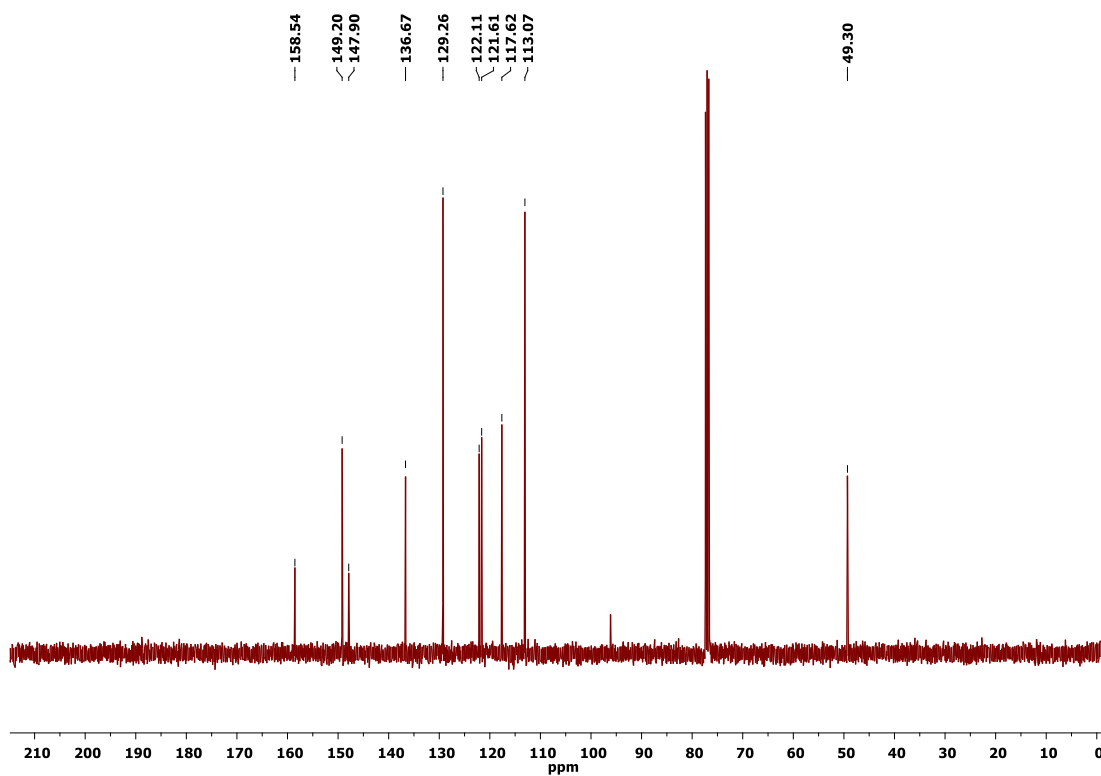


Fig. S2. ¹³C NMR of N-(pyridin-2-ylmethyl)aniline in CDCl₃ at room temperature.

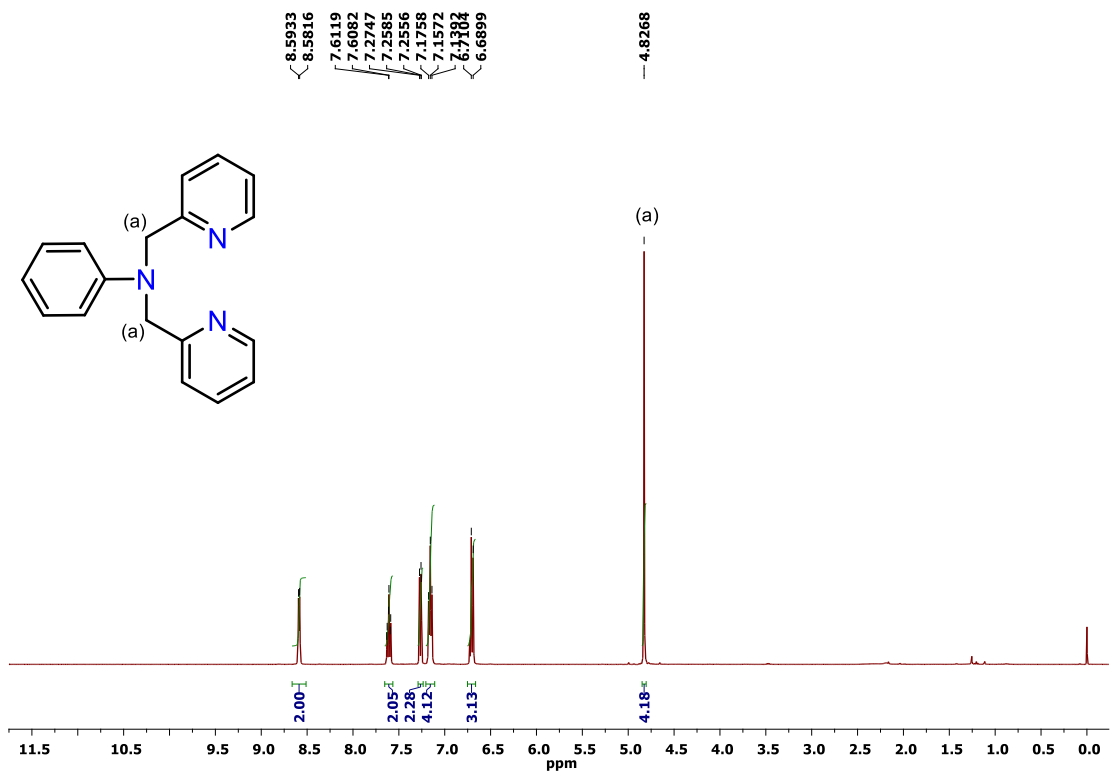


Fig. S3. ¹H NMR of **L** in CDCl₃ at room temperature.

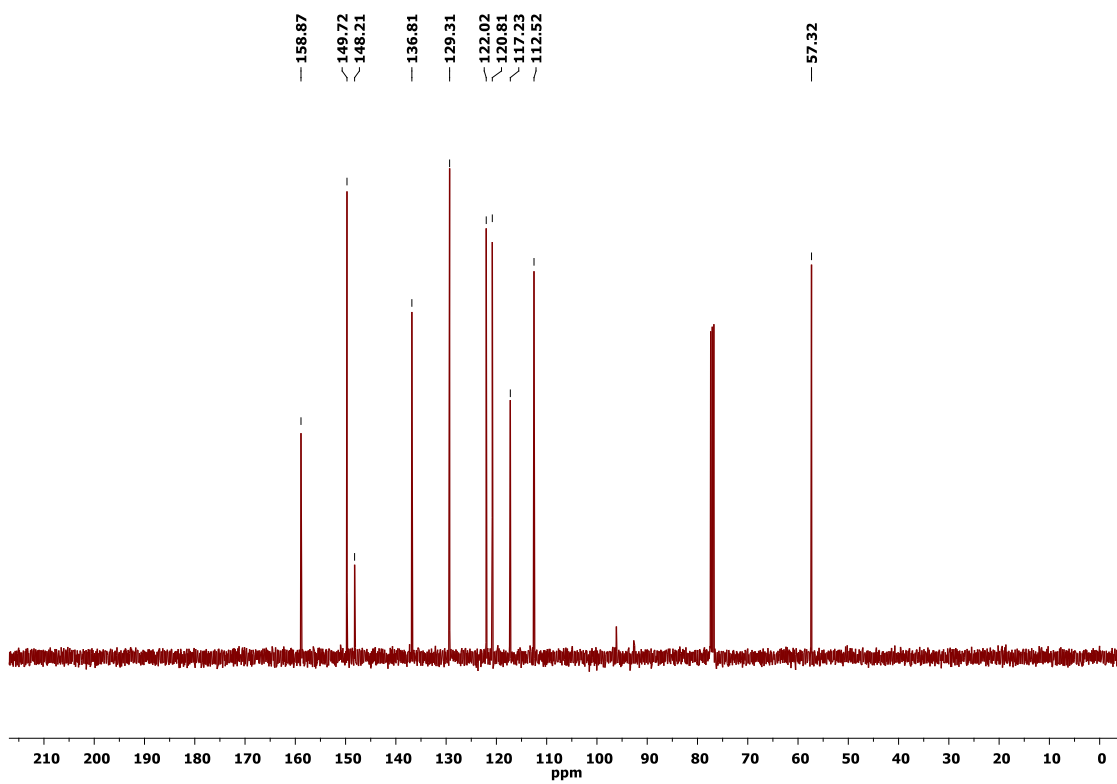


Fig. S4. ¹³C NMR of **L** in CDCl₃ at room temperature.

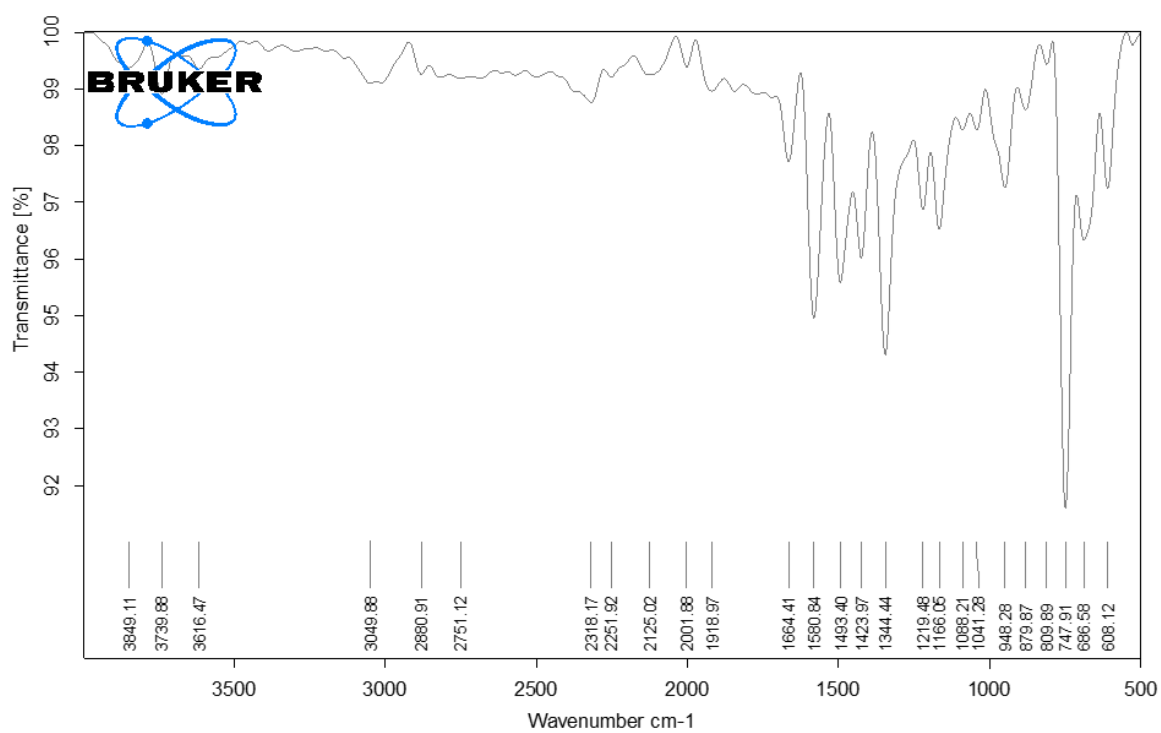


Fig. S5. FT-IR (Solid) spectrum of **L**.

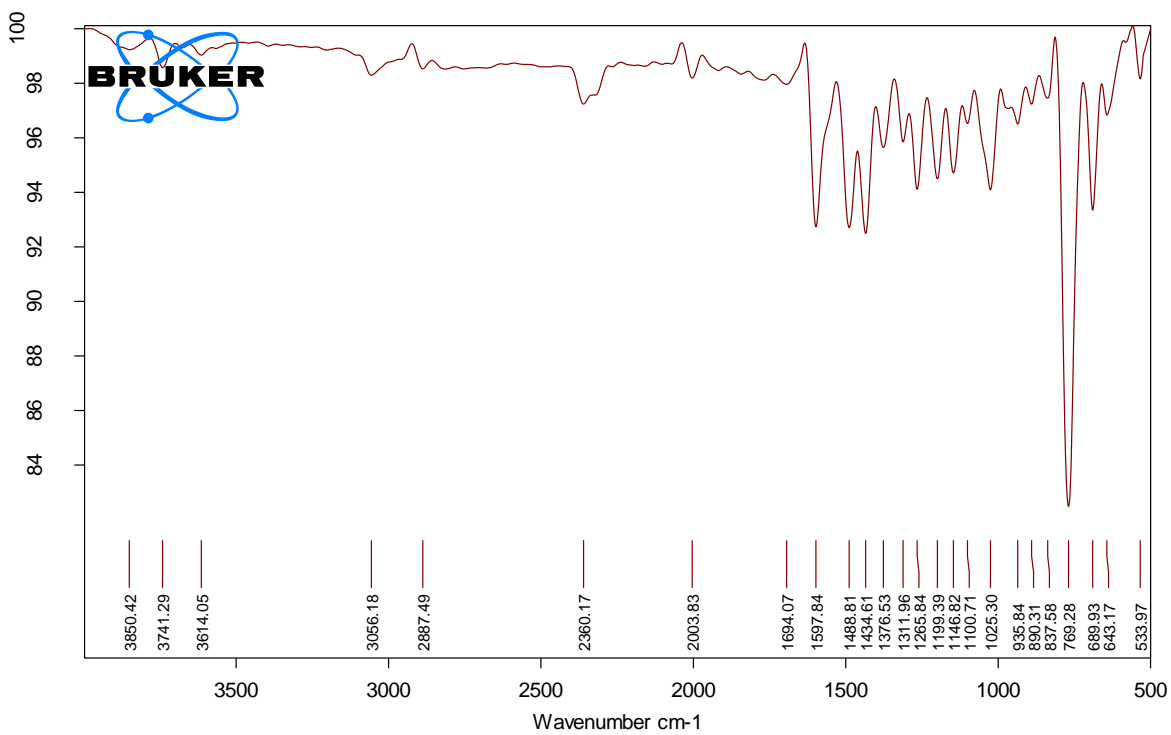


Fig. S6. FT-IR (Solid) spectrum of **1**.

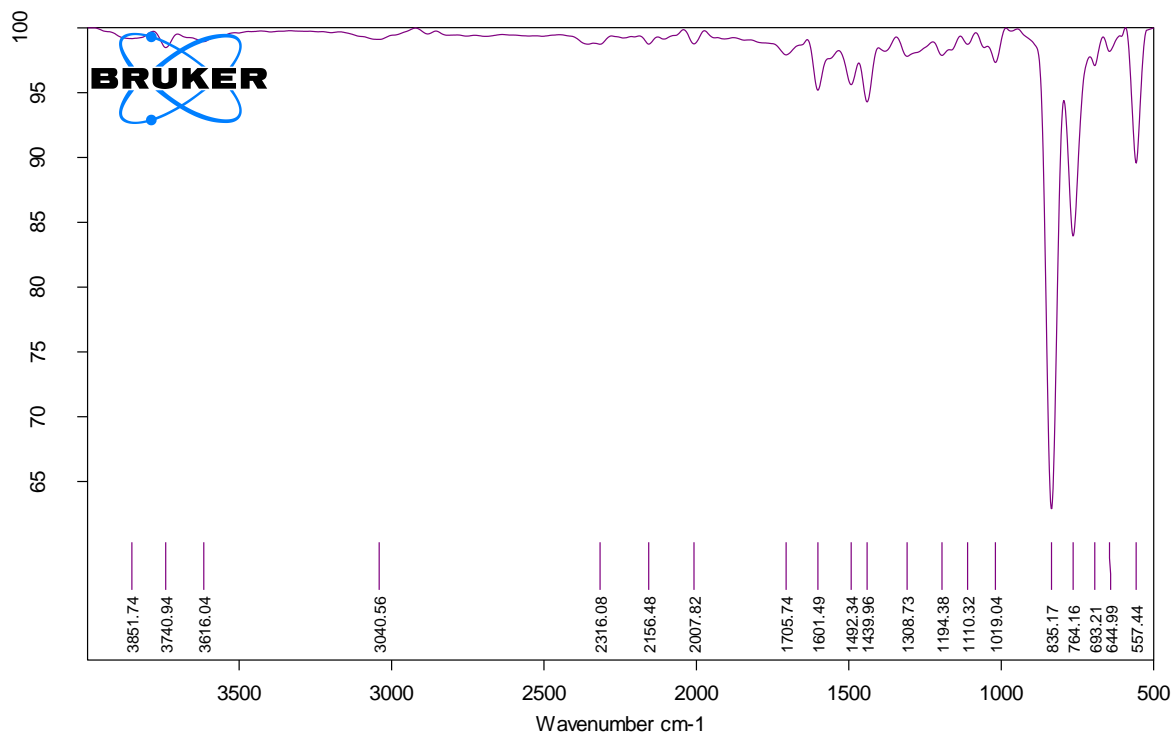


Fig. S7. FT-IR (Solid) spectrum of **2**.

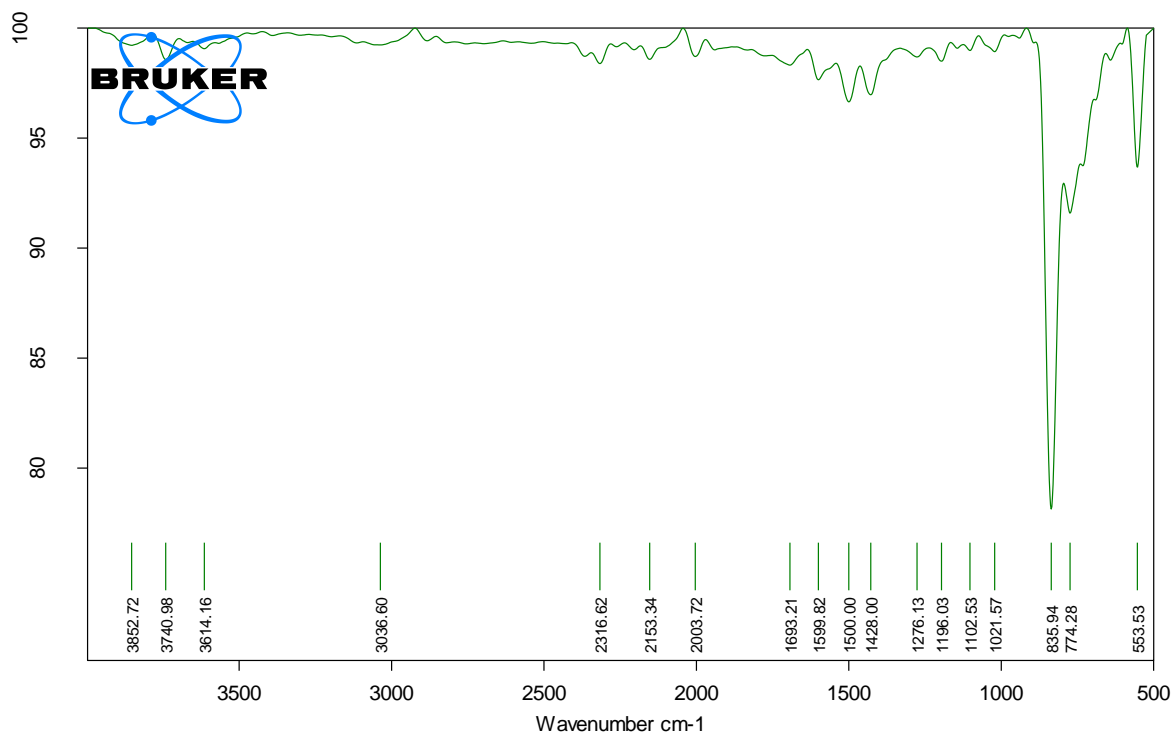


Fig. S8. FT-IR (Solid) spectrum of **3**.

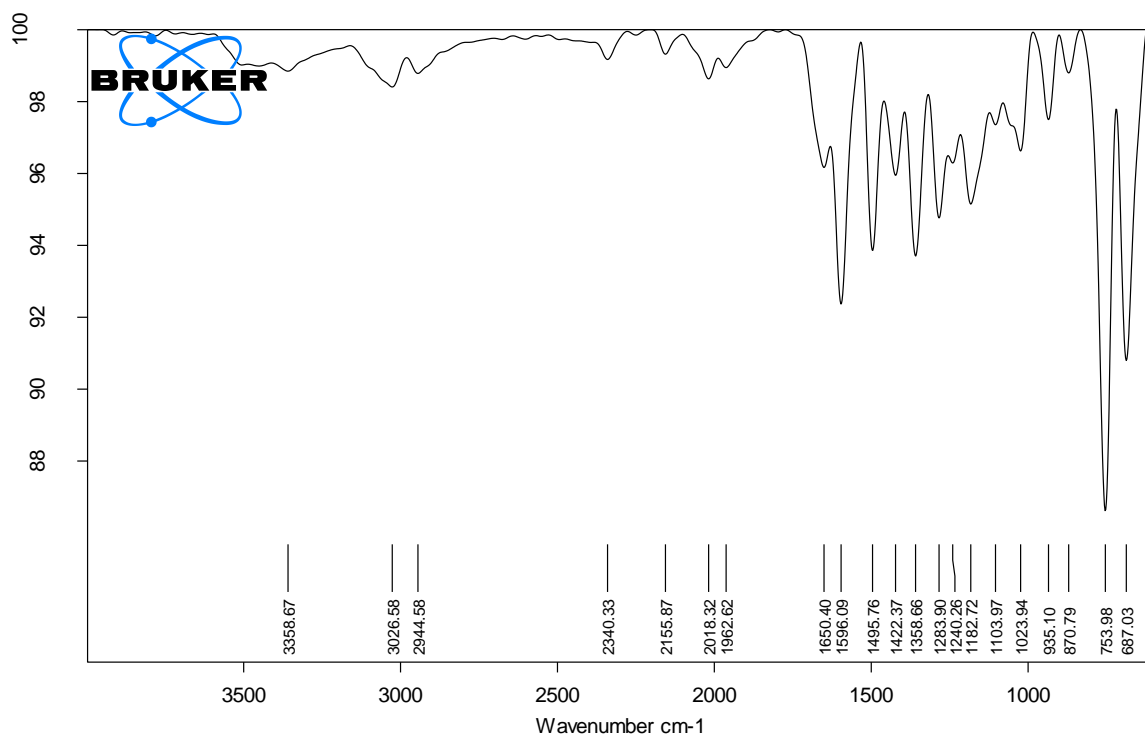


Fig. S9. FT-IR (Solid) spectrum of **4**.

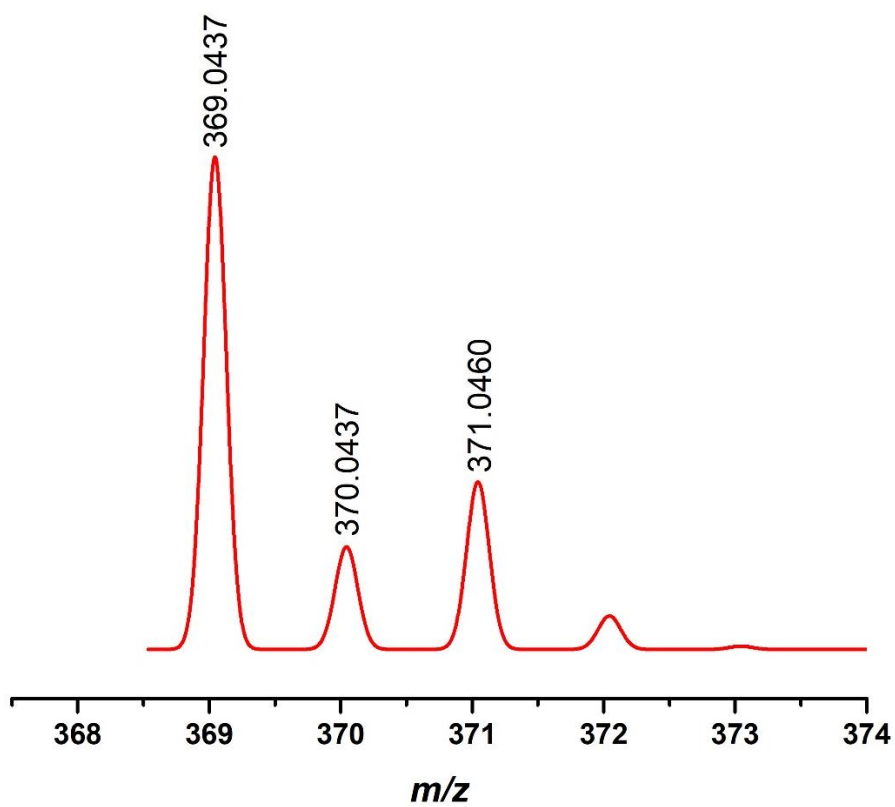
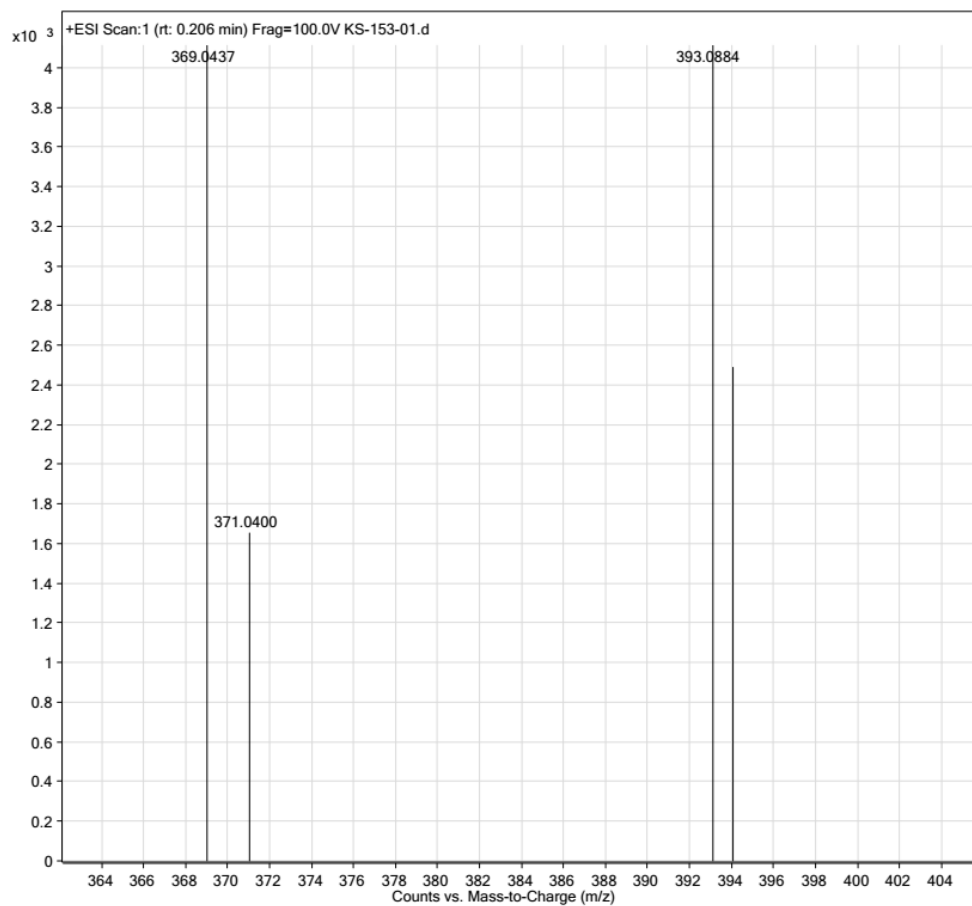


Fig. S10. HRMS spectrum of **1** (top) with their simulated mass spectra (bottom).

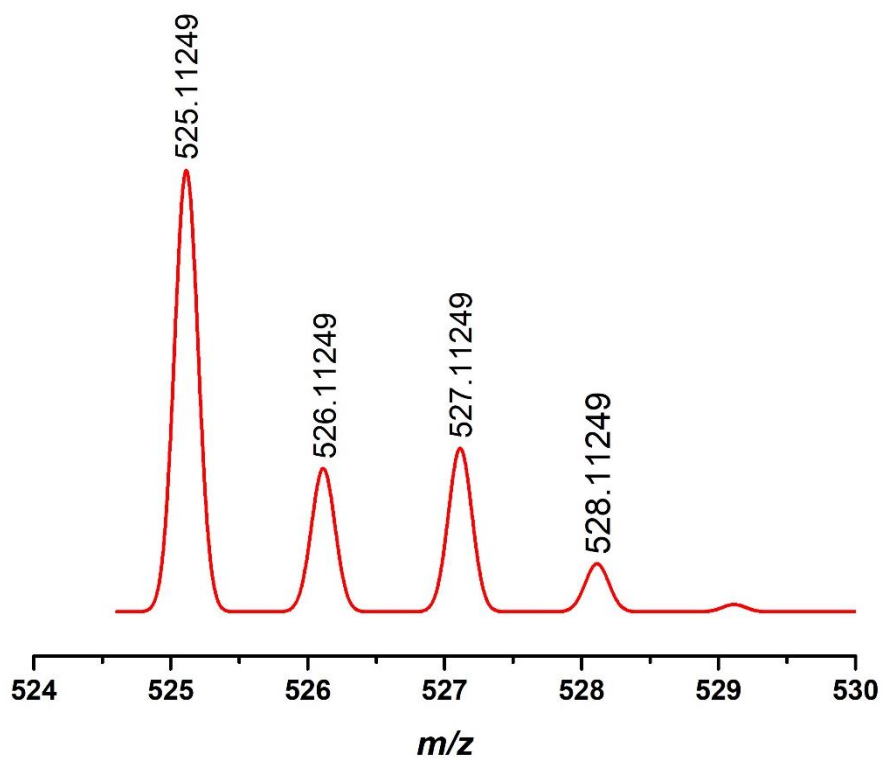
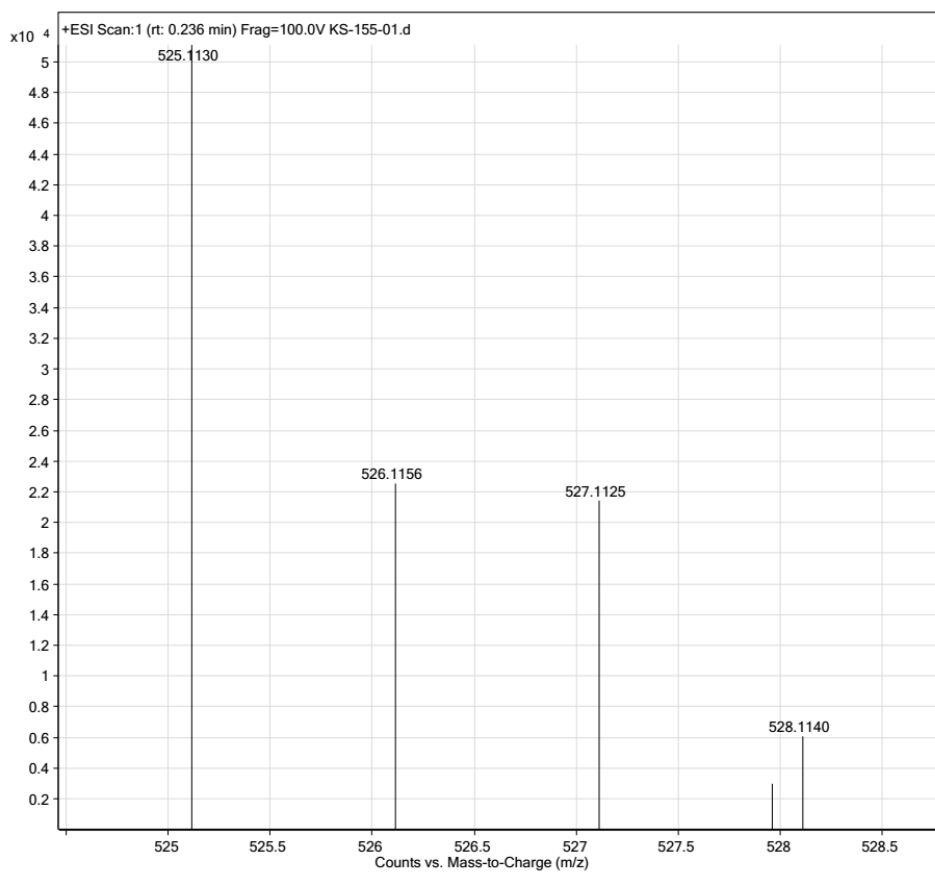


Fig. S11. HRMS spectrum of **2** (top) with their simulated mass spectra (bottom).

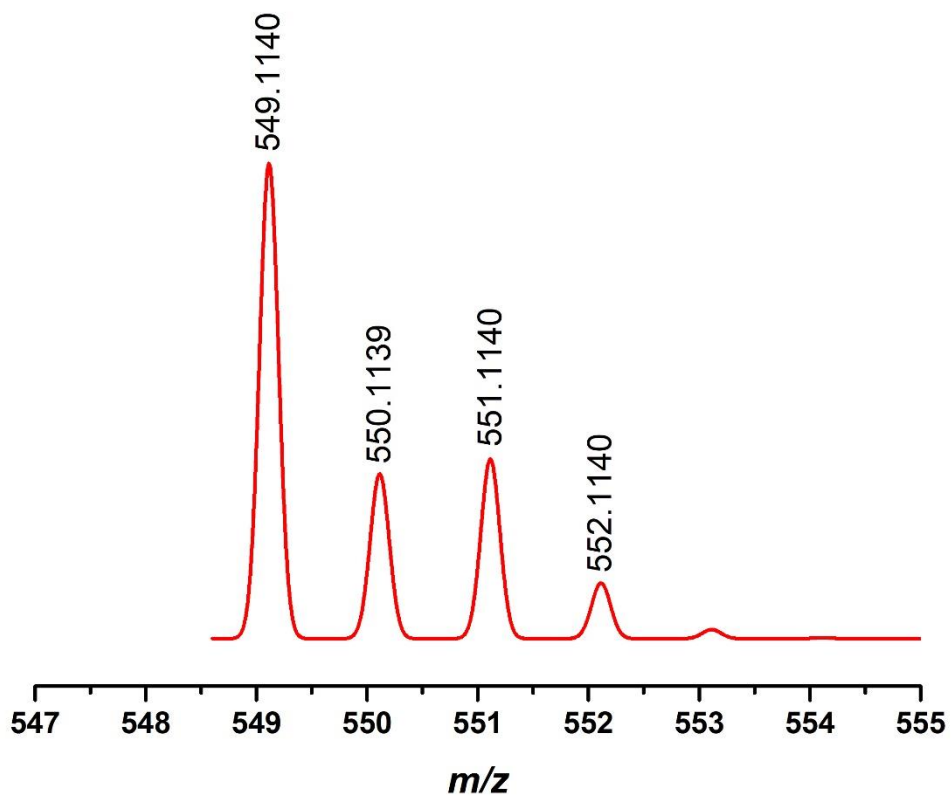
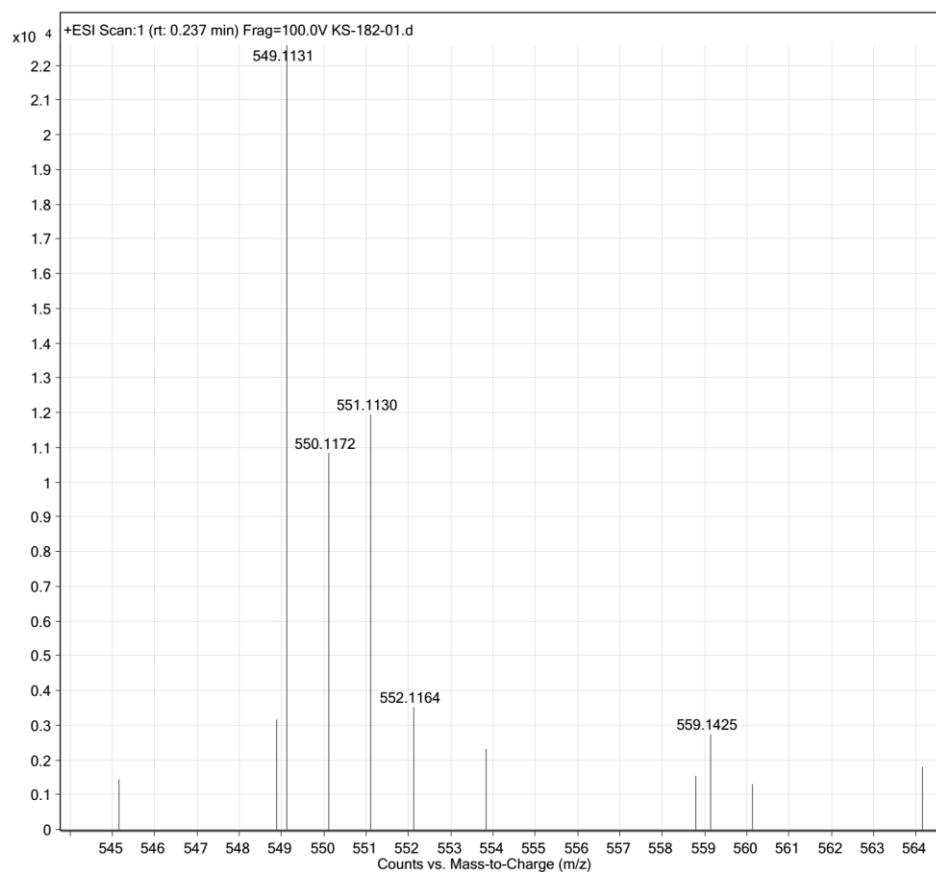


Fig. S12. HRMS spectrum of **3** (top) with their simulated mass spectra (bottom).

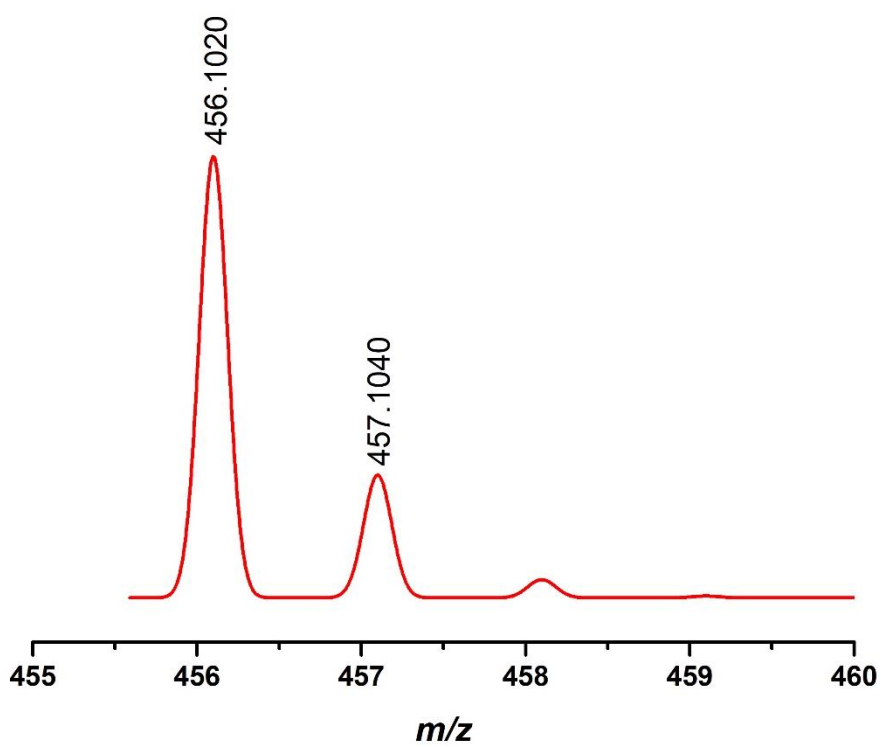
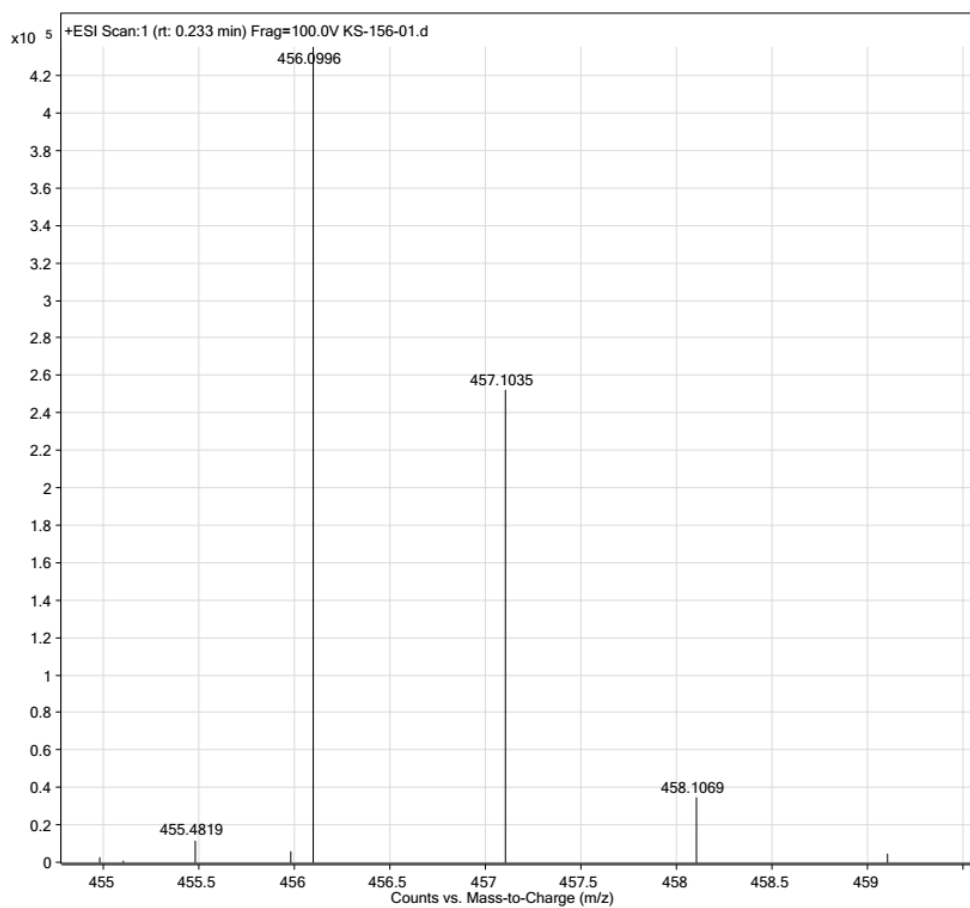


Fig. S13. HRMS spectrum of **4** (top) with their simulated mass spectra (bottom).

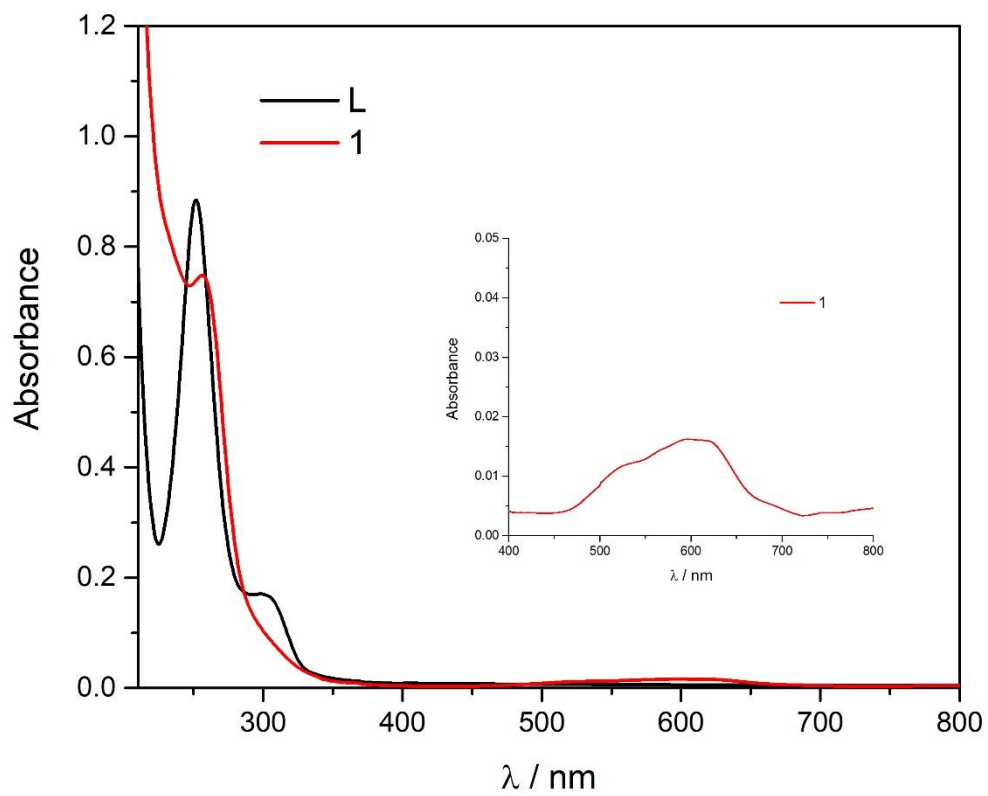


Fig. S14. UV-vis spectrum of L and complexes 1 in acetonitrile.

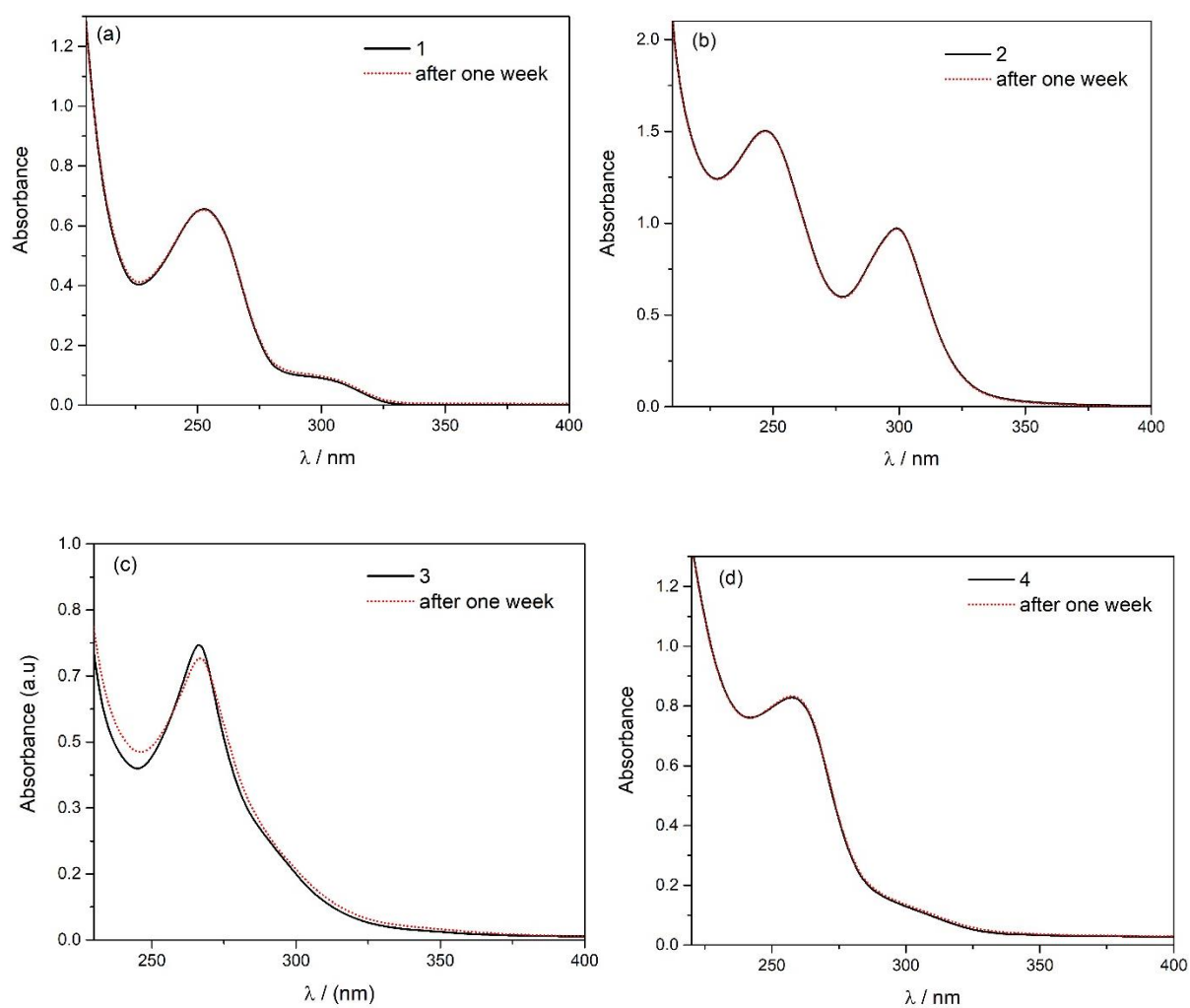


Fig. S15. (a-d) Time dependent UV-vis spectrum of complexes **1-4** in 5 mM Tris-HCl buffer (pH = 7.2) at room temperature.

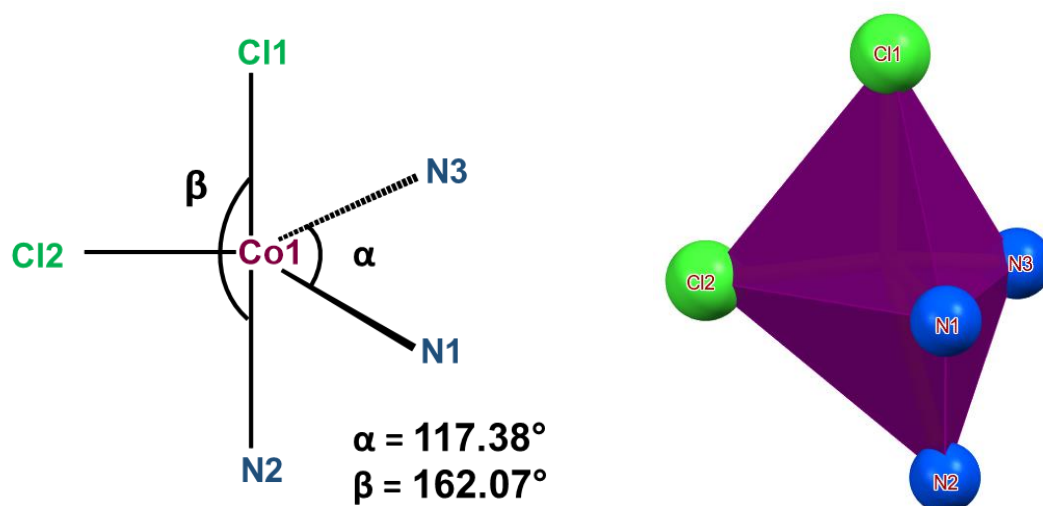
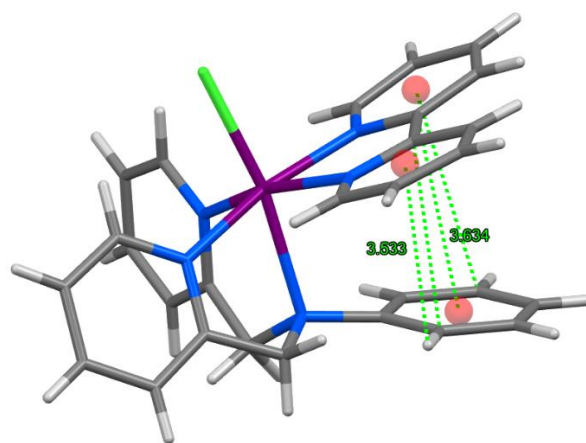
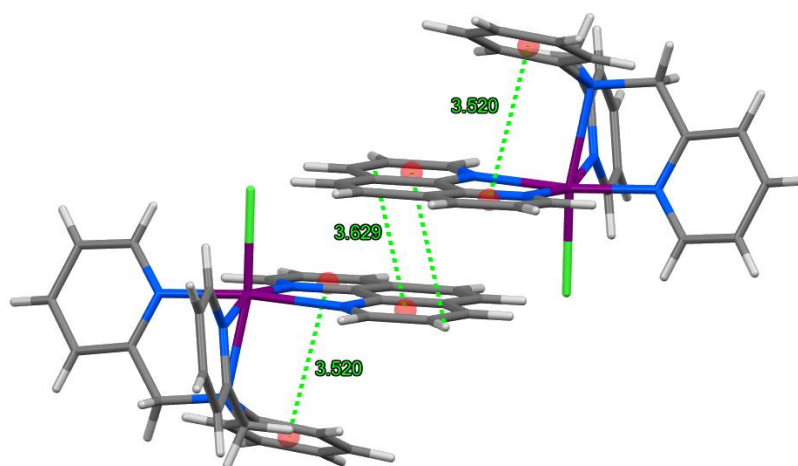


Fig. S16. Schematic drawing of trigonal bipyramidal geometry and polyhedron view of **1**.

a



b



c

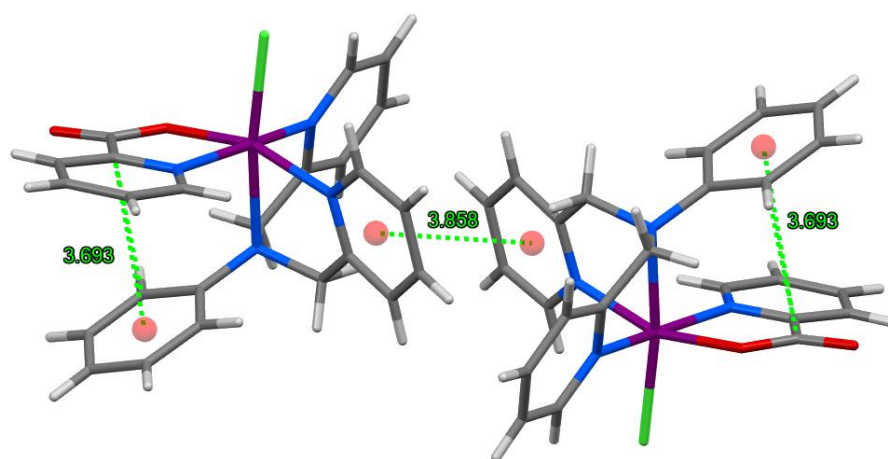


Fig. S17. (a-c) π - π interaction between phenyl group of ligand **L** and bidentate ligands (bpy, phen, pic) in complexes **2-4**, respectively.

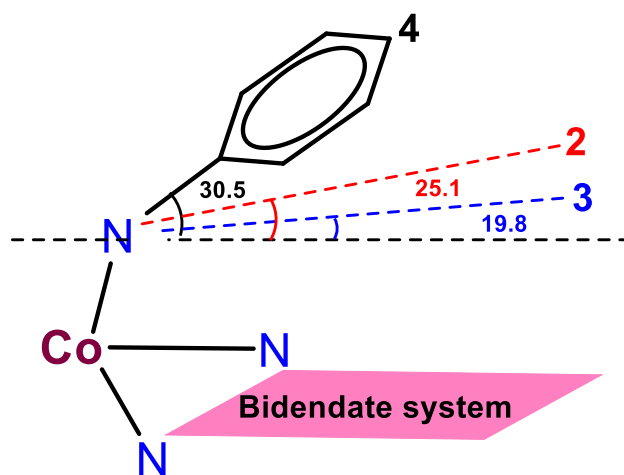


Fig. S18. Schematic drawing of **2–4** with the dihedral angles ($^{\circ}$) benzene ring of **L** and the plane of the bidentate ligand system (bpy, phen and pic).

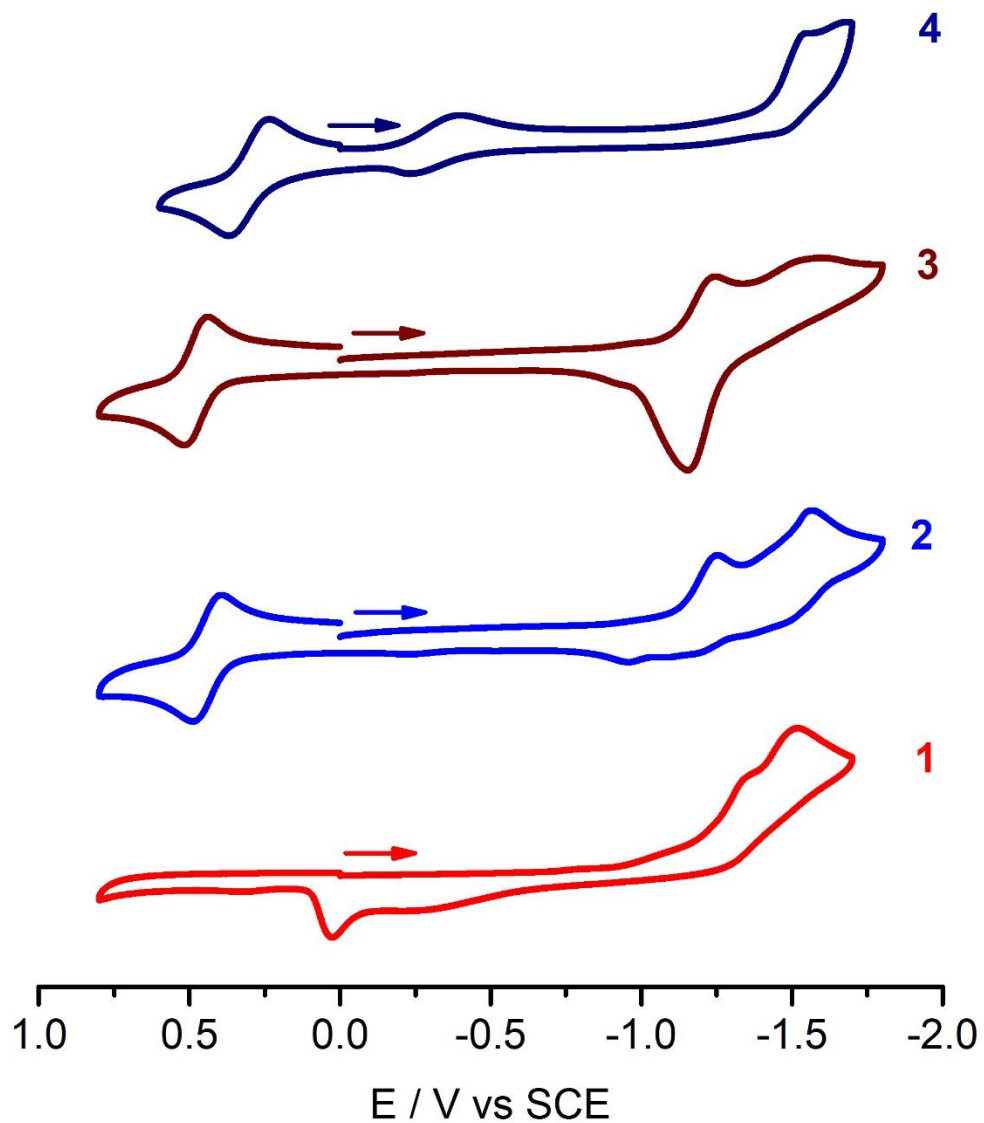


Fig. S19. Cyclic voltammogram of **1–4** (bottom to top) in acetonitrile using 0.1 M TBAP as supporting electrolyte versus SCE, scan rate 100 mV s^{-1} .

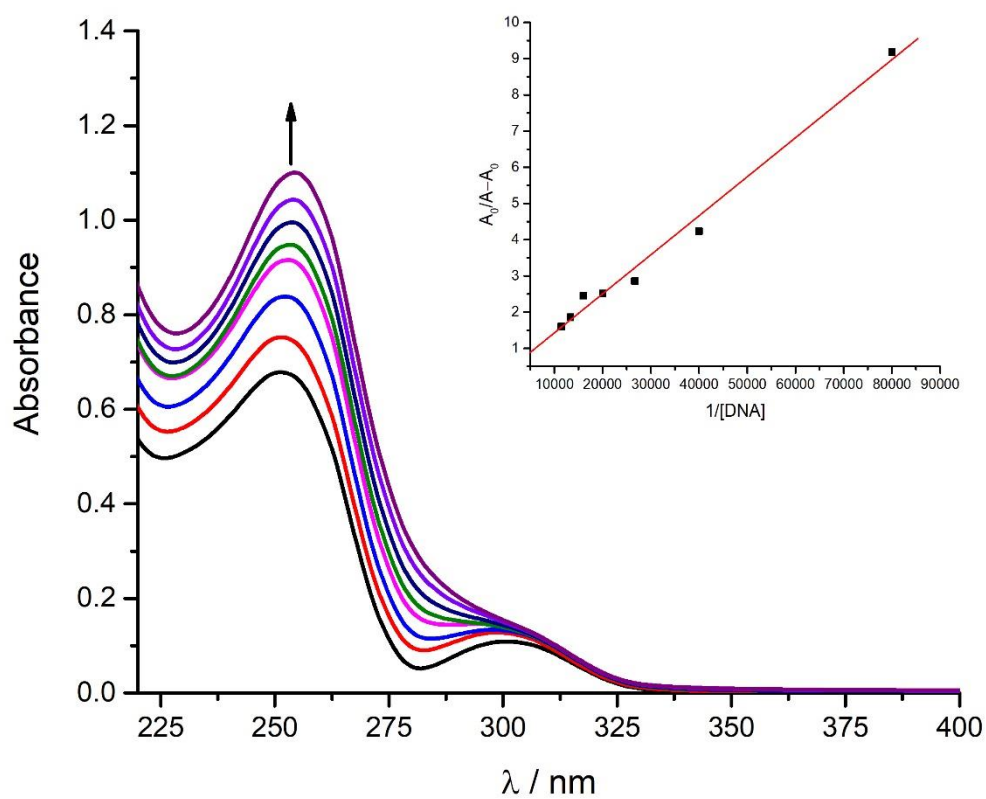


Fig. S20. Absorption spectra of **1** (66.7 μM) in the absence (black) and presence (colour) of ss-DNA (12.5, 25.0, 37.5, 50.0, 62.50, 75.0, 87.5 μM, respectively) in 5 mM Tris-HCl buffer (pH =7.2). The arrow shows the absorbance changes on increasing DNA concentration. Inset: the plot of $A_0/A - A_0$ versus $1/[DNA]$ for the calculation of binding constant of complex **1**.

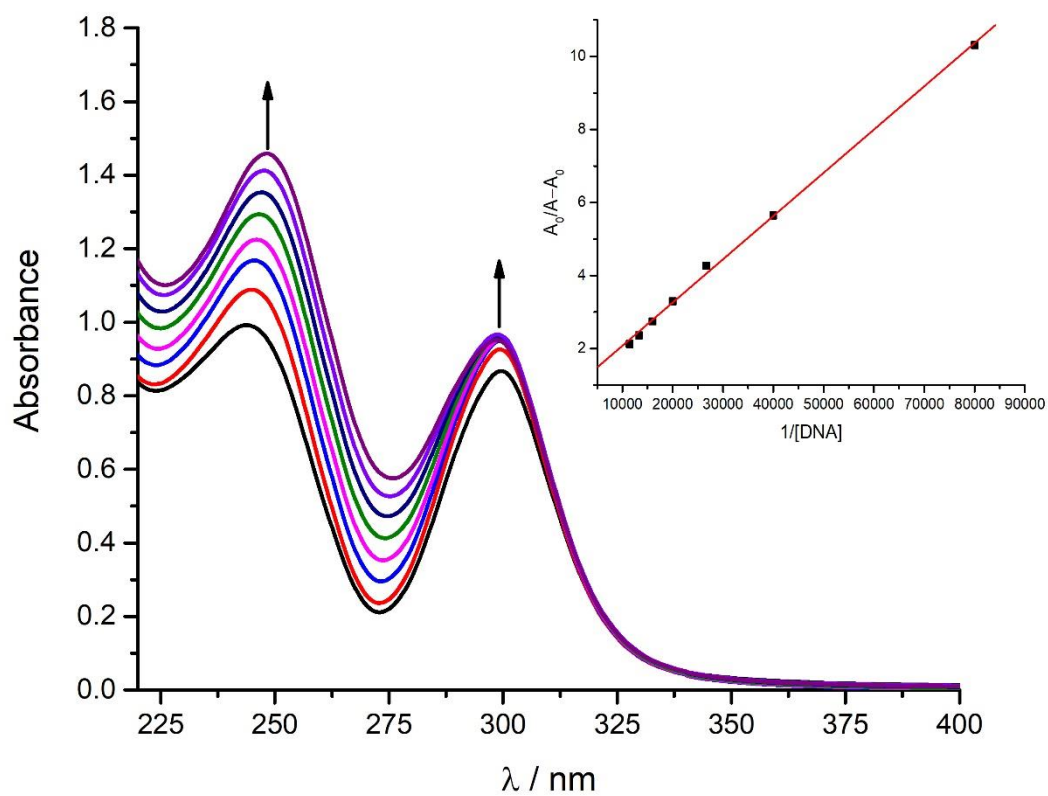


Fig. S21. Absorption spectra of **2** (66.7 μM) in the absence (black) and presence (colour) of ss-DNA (12.5, 25.0, 37.5, 50.0, 62.50, 75.0, 87.5 μM, respectively) in 5 mM Tris-HCl buffer (pH = 7.2). The arrow shows the absorbance changes on increasing DNA concentration. Inset: the plot of $A_0/A - A_0$ versus $1/[DNA]$ for the calculation of binding constant of complex **2**.

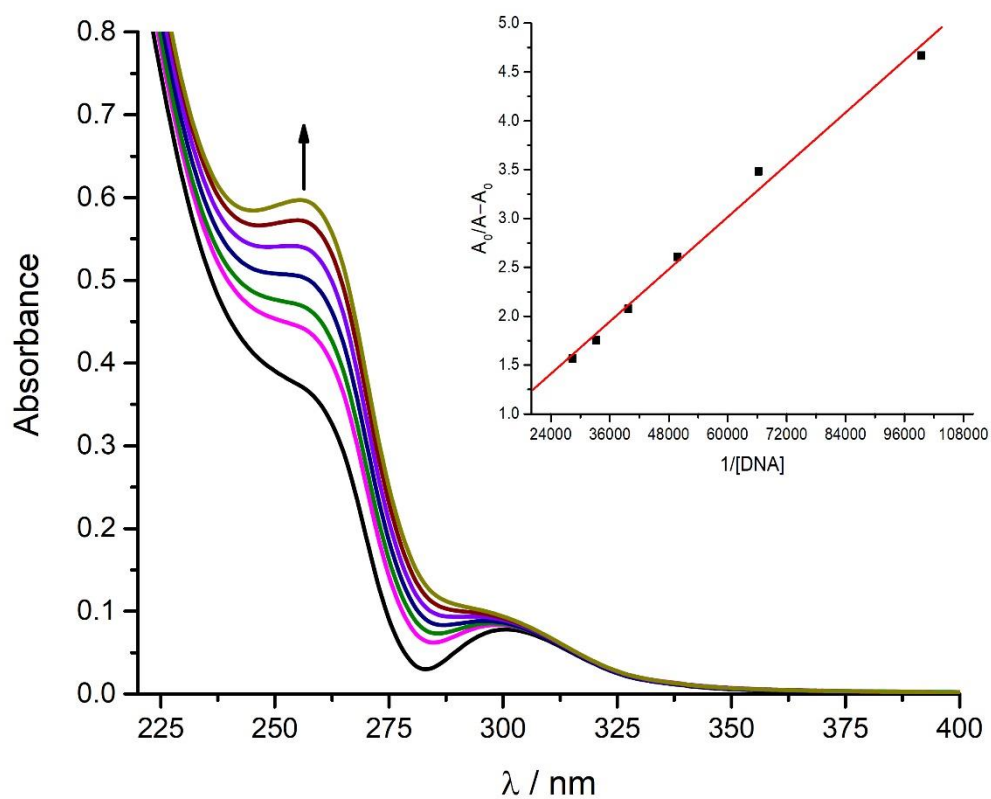


Fig. S22. Absorption spectra of **4** (20 μM) in the absence (black) and presence (colour) of ss-DNA (10.06, 15.09, 20.12, 25.15, 30.18, 35.21 μM, respectively) in 5 mM Tris-HCl buffer (pH =7.2). The arrow shows the absorbance changes on increasing DNA concentration. Inset: the plot of $A_0/A-A_0$ versus $1/[DNA]$ for the calculation of binding constant of complex **4**.

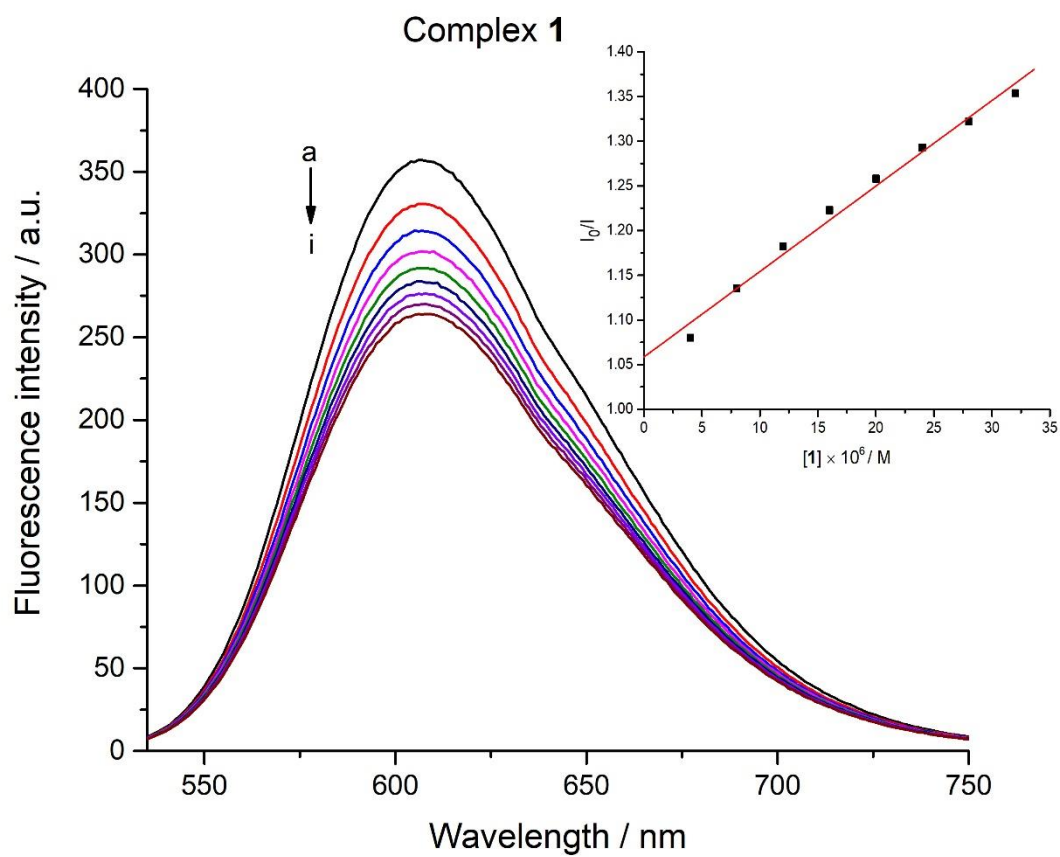


Fig. S23. Emission spectra of EB bound DNA in the presence of **1**. ($[DNA] = 1 \times 10^{-4} M$, $[EB] = 1 \times 10^{-5} M$, $[Quencher](\mu M)$ for **1**: (a) 0, (b) 4, (c) 8, (d) 12, (e) 16, (f) 20, (g) 24, (h) 28, (i) 32. Inset: the plot of I_0/I versus $[Quencher]$).

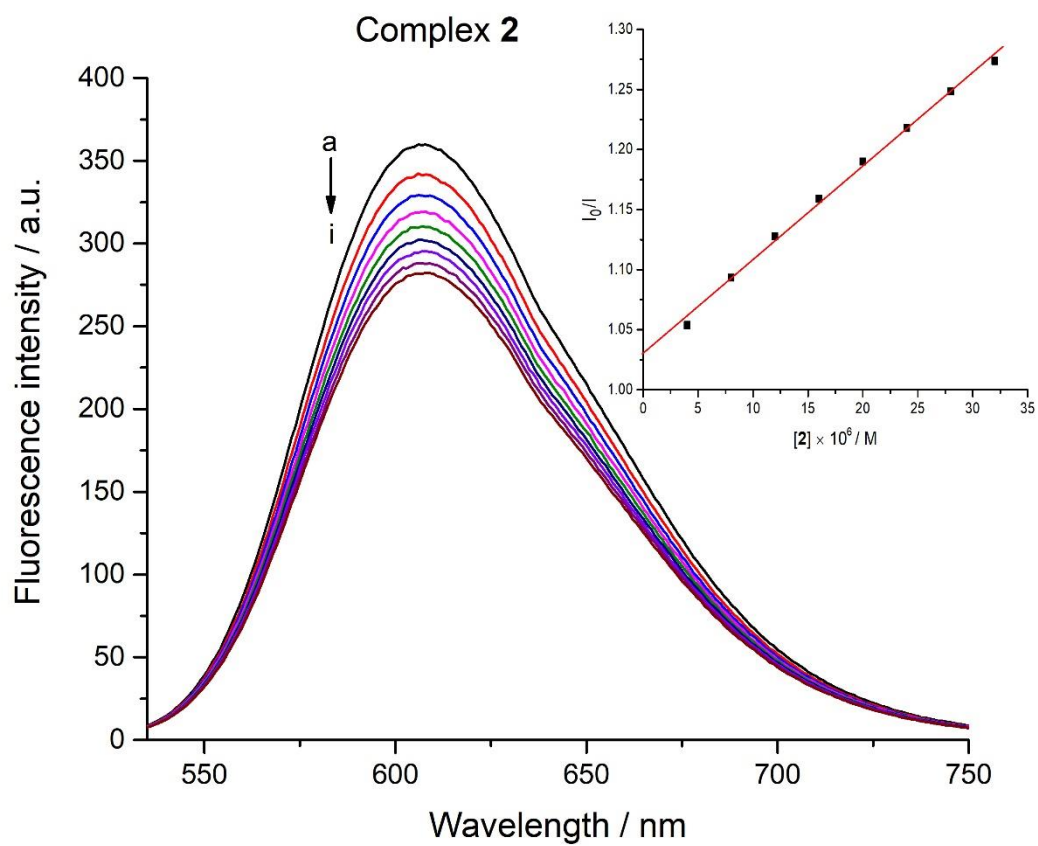


Fig. S24. Emission spectra of EB bound DNA in the presence of **2**. ($[DNA] = 1 \times 10^{-4} M$, $[EB] = 1 \times 10^{-5} M$, $[Quencher](\mu M)$ for **1**: (a) 0, (b) 4, (c) 8, (d) 12, (e) 16, (f) 20, (g) 24, (h) 28, (i) 32. Inset: the plot of I_0/I versus $[Quencher]$).

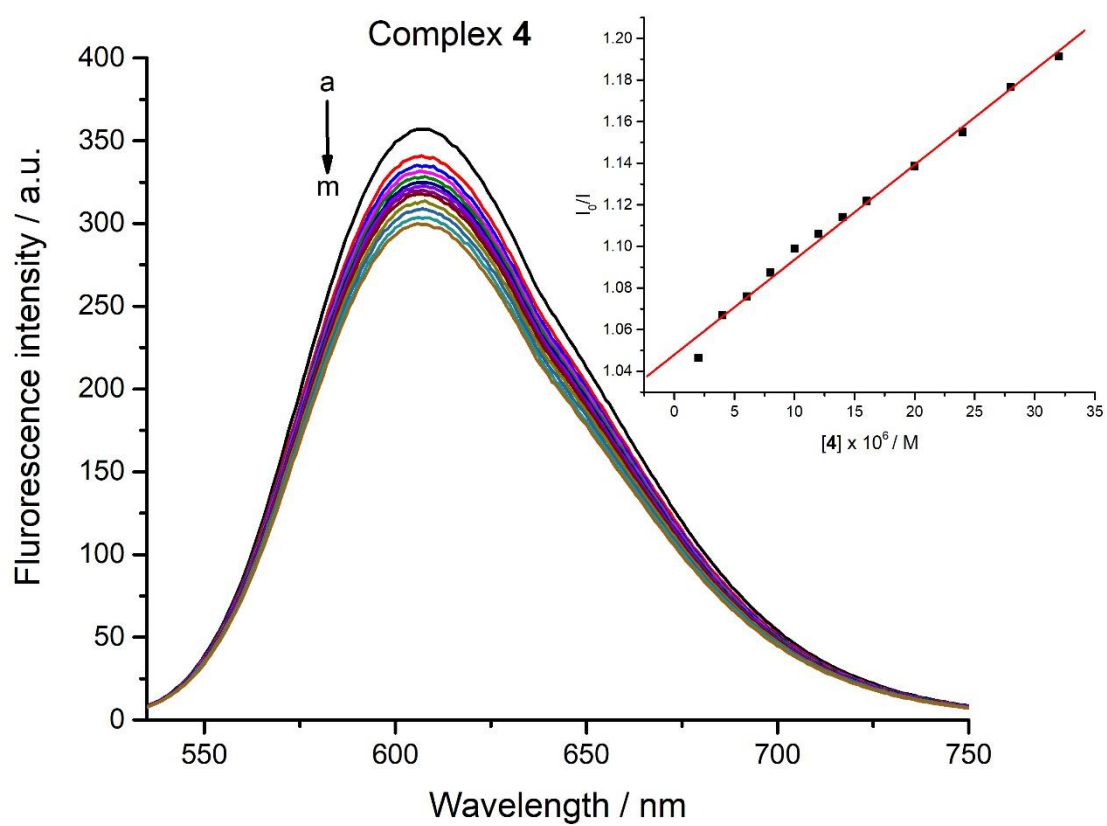


Fig. S25. Emission spectra of EB bound DNA in the presence of **4**. ($[DNA] = 1 \times 10^{-4} M$, $[EB] = 1 \times 10^{-5} M$, $[Quencher](\mu M)$ for **1**: (a) 2, (b) 4, (c) 6, (d) 8, (e) 10, (f) 12, (g) 14, (h) 16, (i) 20, (j) 24, (k) 28, (m) 32. Inset: the plot of I_0/I versus $[Quencher]$).

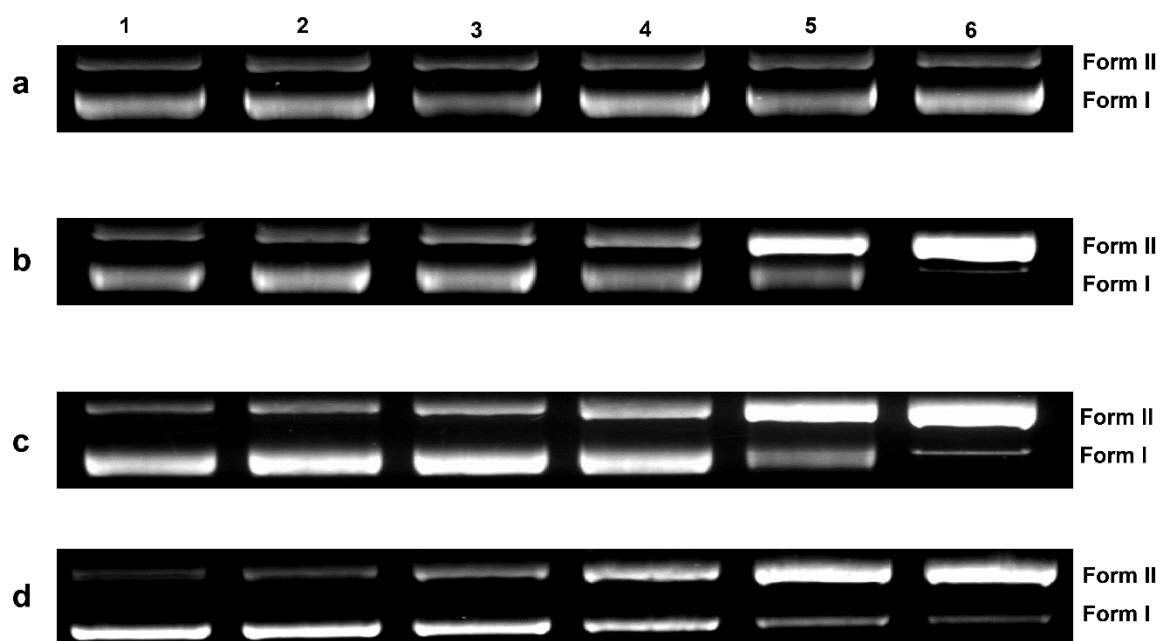
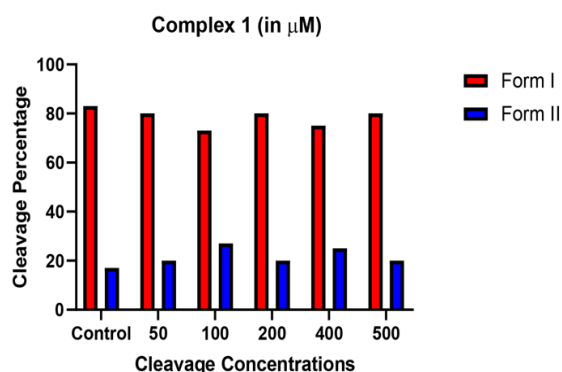


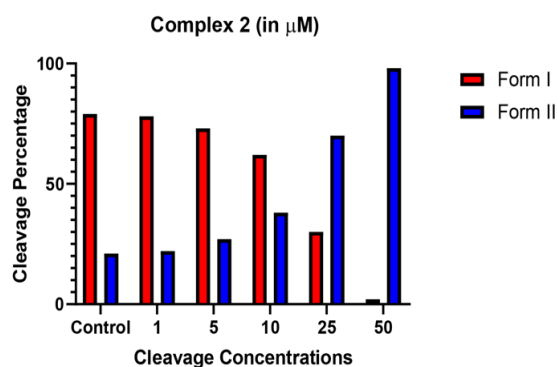
Fig. S26: Agarose gel showing the cleavage of plasmid DNA (pDNA 200 ng/ μ L) at different concentrations upon incubation at 37 °C for 3 h in 50 mM Tris-HCl buffer (pH 7.2). Lane 1: Control; Lane 2-6: pDNA + Complexes [(a) Complex 1: 50 μ M, 100 μ M, 200 μ M, 400 μ M, 500 μ M; (b-c) Complexes 2 and 3: 1 μ M, 5 μ M, 10 μ M, 25 μ M, 50 μ M; (d) Complex 4: 100 μ M, 250 μ M, 500 μ M, 750 μ M, 1 mM].

Table S1: Respective Cleavage Concentrations (1-4) and Percentage of Cleaved Forms of pDNA.

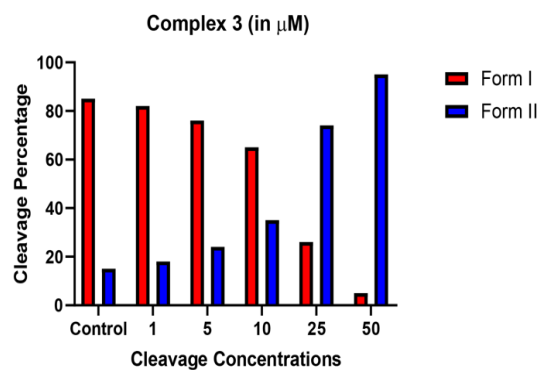
Complex 1			
S.No.	Concentrations (μM)	Form I (%)	Form II (%)
1	Control	83	17
2	50	80	20
3	100	73	27
4	200	80	20
5	400	75	25
6	500	80	20



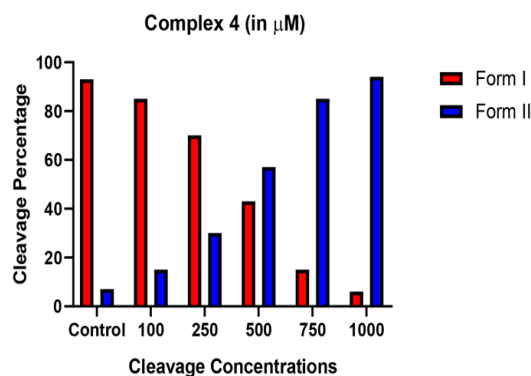
Complex 2			
S.No.	Concentrations (μM)	Form I (%)	Form II (%)
1	Control	79	21
2	1	78	22
3	5	73	27
4	10	62	38
5	25	30	70
6	50	2	98



Complex 3			
S.No.	Concentrations (μM)	Form I (%)	Form II (%)
1	Control	85	15
2	1	82	18
3	5	76	24
4	10	65	35
5	25	26	74
6	50	5	95



Complex 4			
S.No.	Concentrations (μM)	Form I (%)	Form II (%)
1	Control	93	7
2	100	85	15
3	250	70	30
4	500	43	57
5	750	15	85
6	1000	6	94



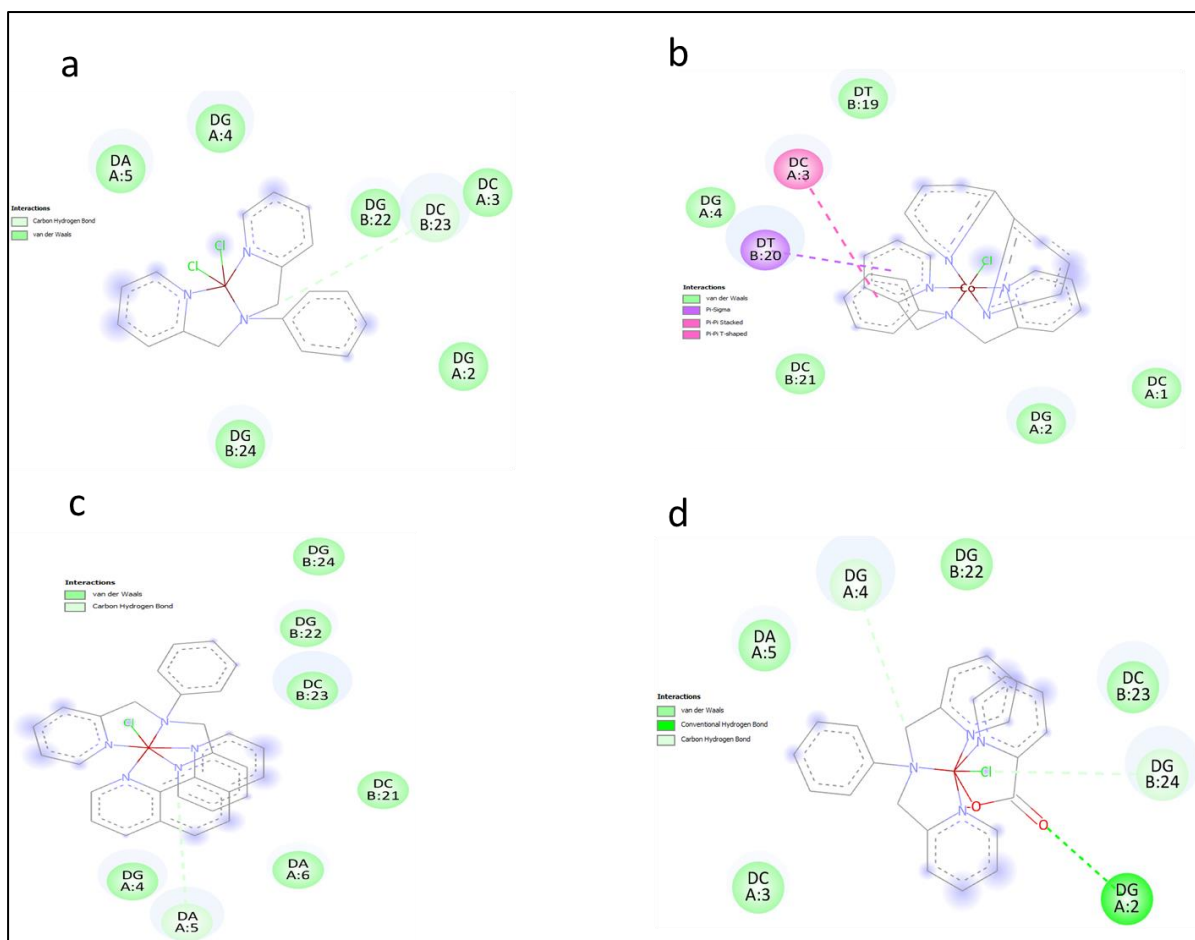


Fig. S27. (a-d) Interactions between complexes (1-4) and DNA, along with the van der Waals forces are represented in a 2-Dimensional format.

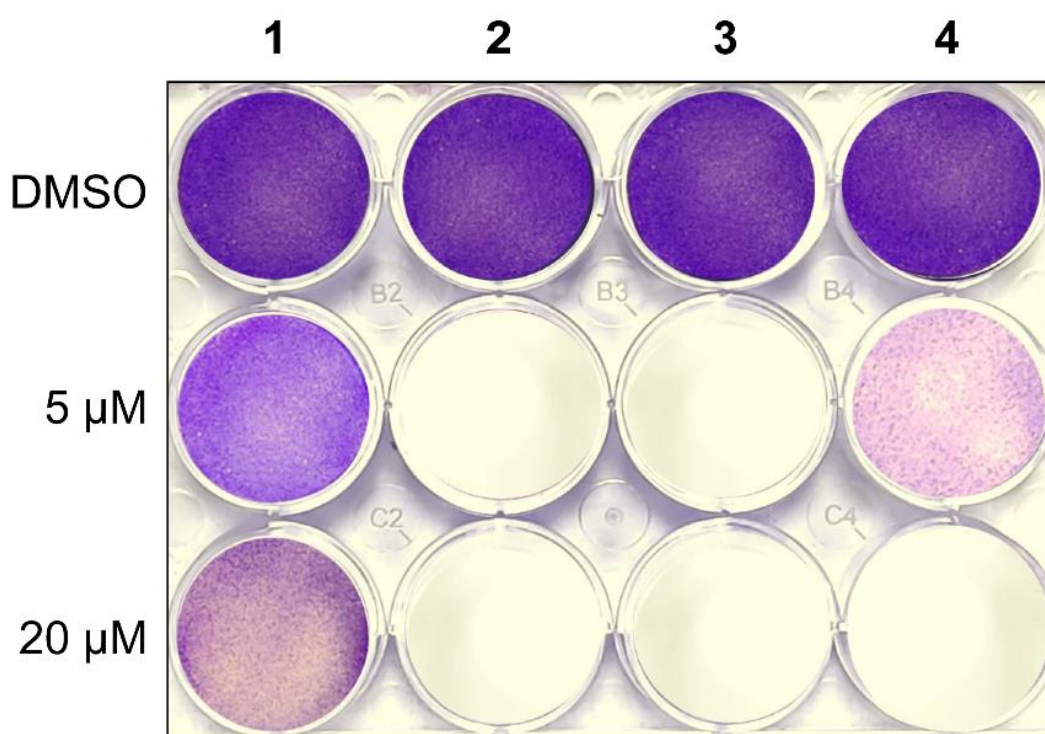
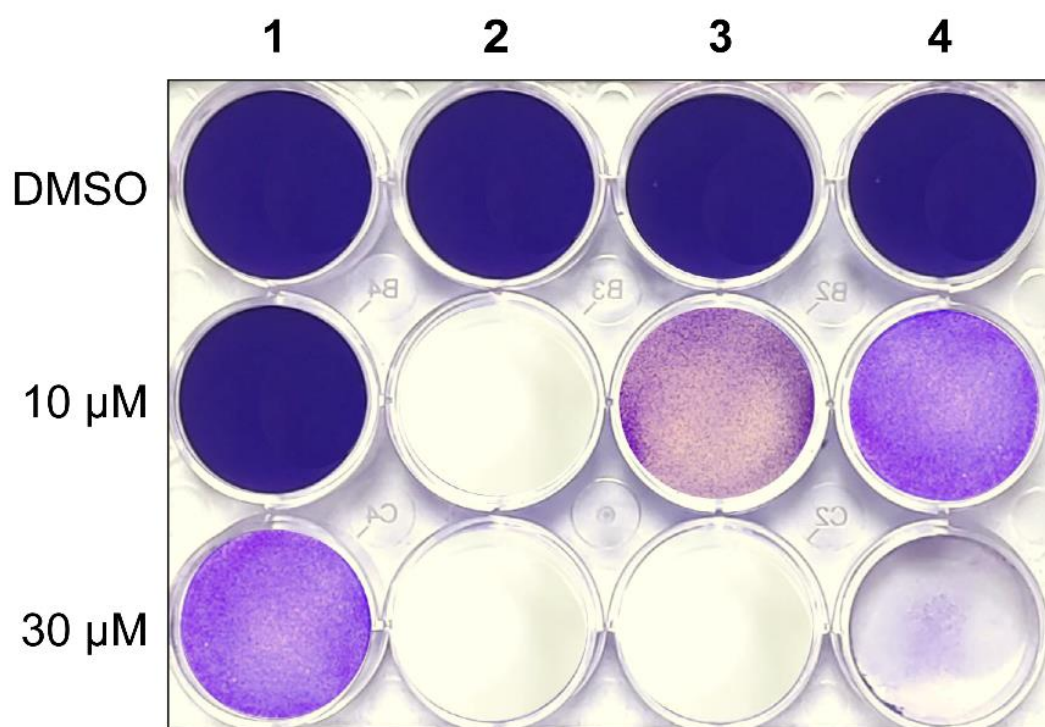


Fig. S28. Crystal violet staining images of A549 cells (top) and MDA-MB-231 cells (bottom) treated with 10 μ M and 30 μ M of **1-4** for 72 h. The purple colour indicates the number of live cancer cells, whereas its loss signifies the decrease in live cells survival.